08

Thermoelectric properties of InGaAs/GaAs quantum dots

© Yu.M. Kuznetsov,[1,2] M.V. Dorokhin,[1] P.B. Demina,[1] N.V. Baidus,[1] A.V. Zdoroveyshchev[1]

[1]Research Institute for Physics and Technology, Lobachevsky State University of Nizhny Novgorod,
603022 Nizhny Novgorod, Russia
[2]Lobachevsky State University,
603022 Nizhny Novgorod, Russia
e-mail: y.m.kuznetsov@unn.ru

Received April 1, 2025
Revised June 16, 2025
Accepted July 3, 2025

The paper presents studies of thermoelectric characteristics of structures representing an array of InAs quantum dots formed on a semi-insulating GaAs substrate by the MOCVD epitaxy method. The theoretical foundations of increasing the thermoelectric efficiency in low-dimensional systems in relation to bulk analogs are described. By comparing the results of measuring the temperature dependences of thermoelectric characteristics and photoluminescence (to estimate the thermal emission of charge carriers), the effect of the quantum dot array on the value of the Seebeck coefficient and specific resistance is demonstrated. It is found that the introduction of a quantum dot array with a sufficiently large nanocluster size into the structure provides an increase in the thermoelectric effect and, accordingly, an increase in the power factor.

Keywords: Thermoelectrics, thermoelectric efficiency, quantum dots, thin films, nanoscale structures.

DOI: 10.61011/TP.2026.01.62851.59-25

Introduction

Thermoelectrics are materials that convert thermal energy into electric one. Efficiency of energy conversion is described by thermoelectric Q factor ZT [1,2]:

$$ZT = \frac{\alpha^2 T}{\rho\lambda} = \frac{PF \cdot T}{\lambda}, \quad (1)$$

where α is a Seebeck coefficient, T is an average temperature of hot and cold sides, $\rho = 1/\sigma$ is resistivity, σ is specific conductivity, $\lambda = \lambda_e + \lambda_{ph}$ is a thermal conductivity coefficient, λ_e and λ_{ph} electron and phonon components of the thermal conductivity coefficient, respectively, $PF = \alpha^2/\rho$ is a power factor.

According to the formula (1), achievement of high thermoelectric efficiency (it is assumed that the values $ZT \geq 1.0$ are high) requires a high value of α and low values of ρ and λ, simultaneously. The main difficulty is that it is impossible to independently control the coefficients α, ρ and λ in bulk solid bodies — an increase of the Seebeck coefficient results in an increase of resistivity. In turn, reduction of ρ according to the Wiedemann–Franz law results in a comparable increase of a contribution by the electron component of thermal conductivity λ_e and, as a result, an increase of λ [1–3].

Today, among the existing low-temperature thermoelectric generators, the record values of ZT belong to semiconductor compounds based on Bi_2Te_3, which was noted already in the studies in the early 90s [1–6]. And, despite the fact that publications that report achievement of ne record values of ZT in these materials still appear up to day, for example [7–10], no substantial progress has been achieved in the increase of ZT for the last 20 years, at least in materials used in the real thermoelectric generators. Primarily, it is due to a weak correlation between demonstrating high efficiency of the material in laboratory conditions and in practice in the real device.

In view of the foregoing, a large practical and fundamental interest has arisen to studying a thermoelectric effect of thin films. The fundamental interest is caused by investigating specific features of thermoelectric phenomena in low-size systems — quantum wells, quantum threads and quantum dots (QD). The practical interest lies in solving a wide spectrum of tasks of powering low-power devices, for which purpose low power of nanostructure generators is enough. As compared to bulk analogues, this type of the generators is advantageous in higher efficiency [1–3]. The recent years have seen more and more studies, which demonstrate applicability of thin thermoelectric films for integration into clothes [11–14], fitness bracelets [15], application of the films to various functional surfaces [16], etc.The thin-film thermoelectrics are actively studied due to an additional degree of freedom that has appeared in them for controlling the magnitude ZT (by varying thicknesses of nanoscale layers). According to a pioneering study [3], selection of the thicknesses in the multi-layer structure allows increasing the value of ZT in up to ten times by independently varying the magnitudes ρ and α (which could increase the conversion efficiency to a level of 60 %).

It is important to note that since for the thin-film samples the heat-transfer processes are decisively contributed by a substrate due to its thickness that is larger relative to the film materials, it is more correct to use the power factor PF instead of ZT for quantitative comparative estimation

of the thermoelectric thin films. It makes possible to evaluate the effective thermoelectric power of the thin-film element, whereas the thermal conductivity characteristics are of secondary importance, since they are determined by a substrate material. We note that the literature deals with usability of the film in isolation from the substrate, which will provide an extremely low thermal flux even when a specific value of λ will be high.

1. Theoretical description of the thermoelectric phenomena in the low-dimensional systems in the $3D$-, $2D$-, $1D$- and $0D$-structures

There is a large number of scientific studies, for example, [1–6,17–20], which report observation of the increased thermoelectric effect in the low-dimensional systems. Causes of an increase of the thermoelectric effect are hidden in specific features of description of kinetics of free charge carriers. According to the study [21], the Seebeck coefficient is determined by a Mott expression:

$$\alpha = \frac{\pi^2 k_b^2 T}{3e} \frac{dln[\sigma(E)]}{/dE}\bigg|_{E=E_F} = \frac{\pi^2 k_b^2 T}{3e}\left(\frac{1}{n}\frac{dn(E)}{dE} + \frac{1}{\mu}\frac{d\mu(E)}{dE}\right)\bigg|_{E=E_F}, \quad (2)$$

where kb is the Boltzmann constant; e is the elementary charge; $\sigma(E)$, $n(E)$, $\mu(E)$ are specific conductivity, a concentration and mobility of free charge carriers having energy of E, respectively; EF is a Fermi energy (level). The equation (2) has used a relationship between the coefficients $\sigma(E)$, $n(E)$, $\mu(E)$, wherein a case of unidirectional n-type conductivity is considered for simplification.

$$\sigma(E) = e \cdot n(E) \cdot \mu(E). \quad (3)$$

It follows from the equation (2) that there are two mechanisms of increasing α. The first one is an increased energy dependence $\mu(E)$, for example, due to a scattering mechanism, which heavily depends on the energy of free charge carriers. And the second one is an increased energy dependence $n(E)$, for example, due to a local increase of a density-of-state function $g(E)$, since the concentration expression is written as:

$$n = 2\int_{E_c}^{\infty} n(E)dE = 2\int_{E_c}^{\infty} f(E,T)\cdot g(E)dE, \quad (4)$$

where $f(E,T) = 1/\Big(1+\exp((E-E_c)/(k_b\cdot T))\Big)$ is a Fermi-Dirac distribution function, E_c is a conduction band bottom. In case of the weak energy dependence of mobility of free charge carriers $d\mu(E)/dE \sim 0$ as well as taking into account (4), the equation (2) will be written as

$$\alpha = \frac{\pi^2 k_b^2 T}{3en}\left(\frac{1}{g(E)}\frac{dg(E)}{dE} + \frac{1}{f(E,T)}\frac{df(E,T)}{dE}\right)\bigg|_{E=E_F}. \quad (5)$$

It follows from the expression (5) that the Seebeck coefficient is determined by a rate of variation of the density of state $dg(E)/dE$ near the Fermi level. Variation of the density of state results in disbalance of the concentration of electrons above and below the level E_F. For example, in metals the density-of-state function weakly depends on the energy, thereby resulting in low disbalance of the concentrations of free charge carriers and, consequently, the low Seebeck coefficient. We note that a sign of $d_g(E)/dE\Big|_{E=E_F}$ determines the sign of the Seebeck coefficient. It is for this reason some metals have a positive coefficient α in the same way as a p-type conductivity semiconductor. We note that the formula (5) is universal in a certain sense — a difference of the bulk structures from the low-dimensional structures lies in a fundamentally different kind of the function $g(E)$. Further consideration requires to specify a kind of the density-of-state function.

Dispersion laws for the bulk semiconductor $(3D) - \varepsilon^{3D}(\mathbf{k})$, the quantum well $(2D) - \varepsilon^{2D}(\mathbf{k})$, the quantum thread $(1D) - \varepsilon^{1D}(\mathbf{k})$ and $KT(0D) - \varepsilon^{0D}(\mathbf{k})$ are written as follows:

$$\varepsilon^{3D}(k_x,k_y,k_z) = \frac{\hbar^2 k_x^2}{2m_x} + \frac{\hbar^2 k_y^2}{2m_y} + \frac{\hbar^2 k_z^2}{2m_z},$$

$$\varepsilon^{2D}(k_x,k_y) = \frac{\hbar^2 k_x^2}{2m_x} + \frac{\hbar^2 k_y^2}{2m_y} + \frac{\hbar^2\pi^2}{2m_z L_z^2} i^2, \ i = 1,2,\ldots \quad (6)$$

$$\varepsilon^{1D}(k_x) = \frac{\hbar^2 k_x^2}{2m_x} + \frac{\hbar^2\pi^2}{2m_y L_y^2} j^2 + \frac{\hbar^2\pi^2}{2m_z L_z^2} i^2, \ i,j = 1,2,\ldots$$

$$\varepsilon^{0D} = \frac{\hbar^2\pi^2}{2m_x L_x^2}\gamma^2 + \frac{\hbar^2\pi^2}{2m_y L_y^2} j^2 + \frac{\hbar^2\pi^2}{2m_z L_z^2} i^2, \ i,j,\gamma = 1,2,\ldots,$$

where k_x, k_y, k_z are components of a wave vector; $\hbar$ is a Dirac constant; m_x, m_y and m_z are components of an effective-mass tensor; L_x, L_y and L_z are typical sizes of a quantum object. In case of dimensionality reduction, the energy is quantized. The dispersion laws (6) result in the following expression of the density-of-states functions [18]:

$$g^{3D}(E) = \frac{1}{2\pi^2\hbar^3}(2m_n^*)^{3/2}(E-E_c)^{1/2},$$

$$g^{2D}(E) = \frac{m_n^*}{\pi\hbar^2 L_z}\sum_i \theta(E-E_i), \quad (7)$$

$$g^{1D}(E) = \frac{\sqrt{2m_n^*}}{\pi\hbar L_y L_z}\sum_{i,j}\frac{\theta(E-E_{ij})}{\sqrt{E-E_{ij}}},$$

$$g^{0D}(E) = \frac{2}{L_x L_y L_z}\sum_{i,j,\gamma}\delta(E-E_{ij\gamma}),$$

where $m_n^* = \sqrt[3]{m_x m_y m_z}$ is an effective mass of the density of states (for electrons); E_i, E_{ij}, $E_{ij\gamma}$ are quantization levels in the quantum well, the quantum thread and the quantum dot, respectively; $\theta(x)$ is a Heaviside function; $\delta(x)$ is a Dirac function.

Substitution of the expressions (7) into the formula (4), and then into (3) makes it possible to obtain analytical expressions of specific conductivity of variously-dimensional semiconductors:

$$\sigma^{3D} = \frac{e\nu}{2\pi^2}\left(\frac{2k_bT}{\hbar^2}\right)^{\frac{3}{2}}(m_x m_y m_z)^{1/2}F_{1/2}(\delta),$$

$$\sigma^{2D} = \frac{e\mu}{2\pi L_z}\left(\frac{2k_bT}{\hbar^2}\right)(m_x m_y)^{1/2}F_0(\xi), \tag{8}$$

$$\sigma^{1D} = \frac{e\mu}{\pi\sqrt{L_y^2 + L_z^2}}\left(\frac{2k_bT^2}{\hbar^2}\right)m_x^{1/2}F_{-1/2}(\eta),$$

where $\delta = \frac{E_F - E_c}{k_bT}$, $\xi = \delta + \frac{\hbar^2\pi^2}{2m_z L_z^2 k_b T}$, $\eta = \delta + \frac{\hbar^2\pi^2}{2m_y L_y^2 k_b T} + \frac{\hbar^2\pi^2}{2m_z L_z^2 k_b T}$ is a reduced chemical potential (relative to the conduction band bottom) in the $3D$-, $2D$- and $1D$-semiconductor, respectively, $F_i(E)$ is a Fermi integral determined by the expression:

$$F_i(E) = \int_0^\infty \frac{x^i dx}{e^{\left(x - \frac{E}{k_bT}\right)} + 1}. \tag{9}$$

Substitution of the expressions (7) into the formula (5) makes it possible to obtain analytical expressions of the Seebeck coefficients of the variously-dimensional semiconductors:

$$\alpha^{3D} = -\frac{k_b}{e}\left(\frac{5F_{3/2}(\delta)}{3F_{1/2}(\delta)} - \delta\right),$$

$$\alpha^{2D} = -\frac{k_b}{e}\left(\frac{2F_1(\xi)}{F_0(\xi)} - \xi\right), \tag{10}$$

$$\alpha^{1D} = -\frac{k_b}{e}\left(\frac{3F_{1/2}(\eta)}{F_{-1/2}(\eta)} - \eta\right).$$

Using the formulas (8) and (10), one can obtain analytical expressions of the power factors PF^{3D}, PF^{2D} and PF^{1D}.

It is not obvious to conclude from an explicit kind of the functions (10) that the Seebeck coefficient increases in the semiconductor due to creation of low dimensionality (formation of the quantum well or the quantum thread). Numerical estimation and comparison of α^{3D}, α^{2D} and α^{1D} requires to consider a specific semiconductor, which is a subject of a separate study and laborious mathematical calculation. For example, the studies [3–6] provide a mathematical calculation based on the formulas (10), which demonstrates the increase of the thermoelectric effect in the materials based on Bi_2Te_3 when reducing dimensionality. Here let us describe general qualitative patterns, which make a fundamental base for demonstrating a principal amplifiability of the thermoelectric effect in the low-dimensional structures as compared to the bulk materials. This qualitative consideration is based on a general kind of the energy dependence of the density-of-states function. The density of states functions are qualitatively shown for all the four cases in Fig. 1.

Thus, in the low-dimensional semiconductor, with a certain value of the Fermi energy E_f the magnitude $dg(E)/dE\,|_{E=E_F}$ can significantly increase, which will result in a significant increase of the Seebeck coefficient according to (5). It is fundamental in this case to technologically select the concentrations of free charge carriers resulting in a required location of the Fermi level as well as to calculate temperature conditions, in which this sample will be operated. Besides, the density of states in a quantum-dimensional layer shall be quite high. Otherwise, variation of the density of states in nanostructured materials will be negligible. Therefore, in practice, amplification of the thermoelectric effect can be reliably recorded only in arrays that include a large number of nanoscale objects within a unit volume (for example, in multi-layer QD arrays).

When analyzing data shown in Fig. 1, *d*, it can be falsely assumed that in terms of achieving extremely high values of the Seebeck coefficient quantum dots are ideal. Indeed, the density-of-states function is a set of delta functions, which will result in huge disbalance of the concentration of electrons above and below the Fermi level when certain conditions are fulfilled. It is worth noting some essential practical limitations. First of all, for the dispersion law shown in Fig. 1, *d*, the large thermoelectric effect is observed in a very narrow temperature range, which is seldom realized in practice. On the other hand, in order to obtain such a dispersion law, the QD array shall have a high degree of homogeneity in sizes. In practice, for the QD arrays obtained by a self-organization method, there is always a Gaussian size distribution, whose width can be quite large. It results in „smearing" of the density-of-states function due to mismatch of dimensional quantization levels in each quantum dot separately. On the one hand, it thus extends a range of temperatures, in which the high thermoelectric effect can be observed. But at the same time, an effect amplitude significantly decreases relative to a maximum value in the homogeneous QD array. Secondly, there is practical uncertainty about an issue of measuring the Seebeck coefficient of a separate quantum dot in isolation from a certain conducting layer, which is necessary to provide the quantum dot with new carriers instead of those that left the quantum dot area due to thermal interaction. It is for this reason the formulas (8) and (10) there are not expressions for the QD case. Thus, an increasability of a final value of ZT is not obvious a priori, but shall be experimentally confirmed for each specific system.

2. Sample manufacturing technology

According to the foregoing, the present study was aimed at experimentally checking amplifiability of the thermoelectric effect by introducing the arrays of the

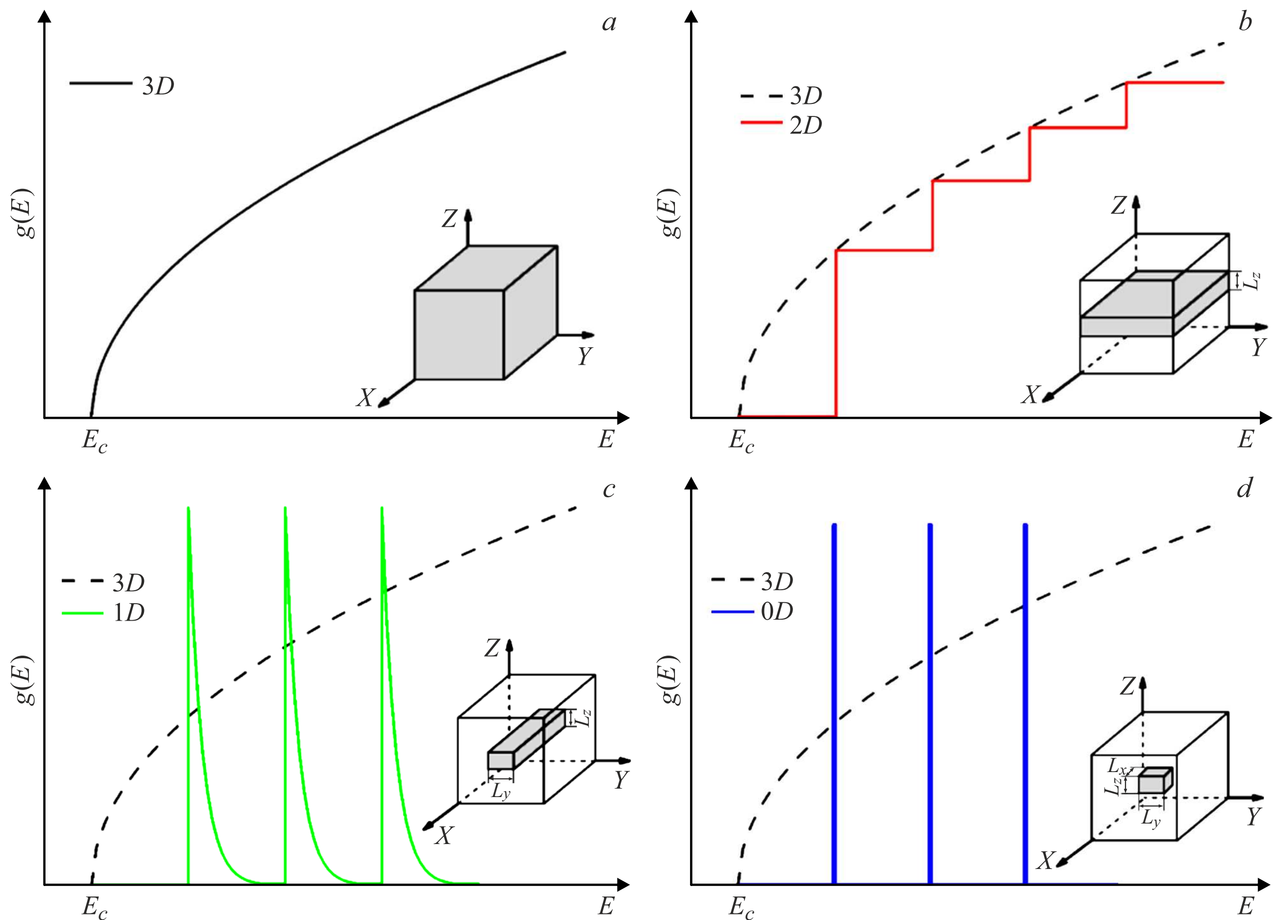

Figure 1. Density-of-states function in case of the: *a* — 3*D*, *b* — 2*D*, *c* — 1*D*, *d* — 0*D* semiconductor.

self-organized quantum dots into a semiconductor matrix. For this purpose, we have formed and studied the thin thermoelectric films based on heterostructures containing the In(Ga)As/GaAs quantum dots. The samples were formed on the substrate of a semi-insulating GaAs by vapor-phase epitaxy in an AIX-200RF installation at the reduced hydrogen pressure. It is obvious that the contribution by the quantum-dimensional layer to the thermoelectric effect increases with an increase of their number. Therefore, in order to obtain a signal exceeding a measurement error and a value of a technological spread, it is necessary to form multi-layer structures. For this reason, the studied structure was 10 thin (3 nm) $In_xGa_{1-x}As$ ($x \approx 0.5$) layers separated by GaAs spacer layers In terms of dimensional quantization, the layers were a hybrid system, which included a $In_xGa_{1-x}As$ quantum well ($x < 0.5$), above which a high-density array of the $In_xGa_{1-x}As$ quantum dots ($x > 0.5$) was formed. Such systems were described in the study [22]. The multi-layer array was formed between the heavily-doped-GaAs layers of the thickness of 150 nm (below) and 80 nm (above). In the present study, a variable parameter was a layer application temperature (T_g). Besides, we also formed a reference multi-layer structure, in which instead of the quantum well+QD layers the homogeneous layers of the $In_{0.3}Ga_{0.7}As$ quantum wells were formed, while the other parameters (thickness, a doping level) remained unchanged. A total thickness of the epitaxial layers in all the samples was 860 nm. The samples are schematically drawn in Fig. 2, *a*. The sample list is given in Table 1. A study of specific features of growth of such structures as well as description of their transport and optical properties are provided in more detail in the studies [23–26].

The GaAs substrates are selected for forming the QD structures due to their compatibility with the InGaAs system as well as good electrical insulation properties of gallium arsenide that has room temperature's resistivity at the level of 10^9 Ω·cm. Such a high value (which is by several orders higher than the layer resistance) excludes the influence of the substrate on measurements of the thermoelectric characteristics of the films for the operating temperature up to 300 °C (details will be discussed below). The InGaAs system is selected for studying the QD influence on the thermoelectric properties due to a high degree of development of the technology of manufacturing of the QD arrays, including the multi-layer ones, which are necessary for reliably recording the thermoelectric effect. The optical, electrical and structural properties of the In(Ga)As/GaAs

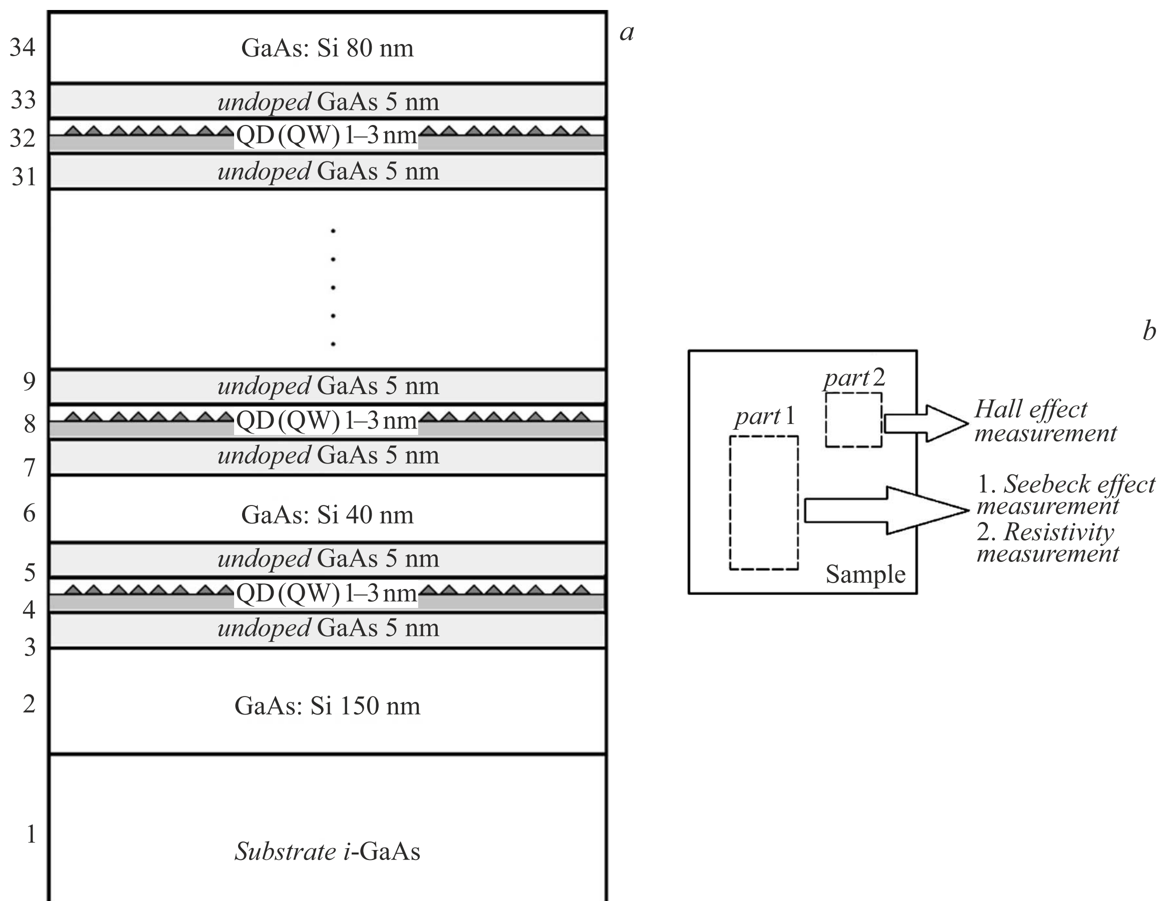

Figure 2. *a* — a schematic image of the samples, the samples 2 – 4 had quantum dots (QD) formed, the sample 1 had quantum wells (QW) formed, *b* — a scheme for splitting the samples into two parts: the first one was used form measuring the Hall effect, the second one was used for measuring the Seebeck coefficient and resistivity.

Table 1. List of the studied samples

№	n_{hall}, cm^{-3}	Description	Growth temperature
1	$6.5 \cdot 10^{18}$	Reference sample, 10 quantum well layers	For all the layers $T_g = 650\,^\circ$C
2	$6.5 \cdot 10^{18}$	10 QD layers above the InGaAs	quantum well The quantum well layer+QD at $T_g = 550\,^\circ$C Layers of GaAs $T_g = 650\,^\circ$C
3	$6.5 \cdot 10^{18}$	10 QD layers above the InGaAs	quantum well quantum well layer+QD at $T_g = 530\,^\circ$C Layers of GaAs $T_g = 650\,^\circ$C
4	$1.3 \cdot 10^{19}$	10 QD layers above the InGaAs	quantum well quantum well layer+QD at $T_g = 520\,^\circ$C Layers of GaAs $T_g = 650\,^\circ$C

quantum dots have been previously investigated by us in a series of the studies [23,27–29]. We also note the study [30], which has discussed use of the InGaAs structures as thermoelectric sensors.

For the tests, the deposited-layer sample was cut to obtain a piece of sizes 5×5 mm for estimating the concentration of charge carriers by the Hall effect measurements as well as a piece of sizes 5×10 mm for measuring the thermoelectric characteristics (Fig. 2, *b*): the Seebeck coefficient and resistivity (these parameters were measured at the same part of the sample). Table 1 specifies a Hall concentration of free charge carriers (n_{hall}), which is measured at the room temperature.

3. Experimental procedure

The most important component of analysis of the QD structures is estimation of energy characteristics: studying the states localized at the dimensional quantization levels

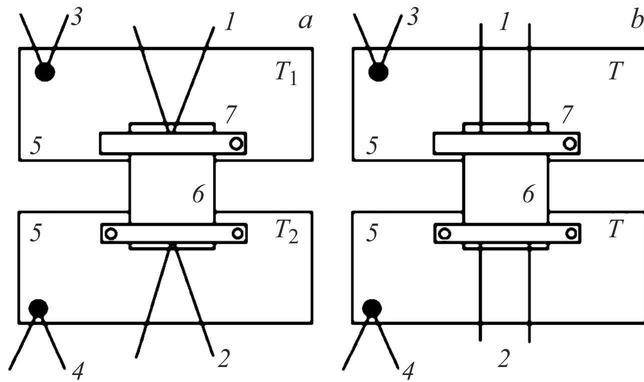

Figure 3. *a* — a diagram for measurement of the Seebeck coefficient: *1*, *2* — measurement thermocouples; *3*, *4* — thermocouples designed to control a temperature of heating tables *5*; *6* — a sample; *7* — graphite clamps; *b* — a diagram of measurement of resistivity: *1*, *2* — measurement wires.

in the quantum dots. For this purpose, photoluminescence (PL) spectra of the formed structures have been measured. The measurements are within the temperature range 10 – 330 K using a closed-cycle helium cryostat. Luminescence was excited by radiation of a He-Ne-laser with the wavelength of 0.63 μm, power of 15 mW and a beam diameter of 1 mm. Radiation was collected at a front side of the sample, focused to an entrance slit of an MDR-2 monochromator and recorded by the InGaAs-detector. Based on the obtained PL spectra, a temperature dependence of PL integral intensity was constructed.

Procedures of measurements of the thermoelectric properties (the Seebeck coefficient, resistivity) were realized based on a VUP-4 installation. The sample was installed onto graphite furnaces, which were heated by radiation of KGM-100 halogen lamps. The furnaces are installed in a vacuum chamber with residual vapor pressure of at most 10^{-5} Torr. A thermo-EMF was measured by means of K-type thermocouples and a data collection system L-CARD E14-140-MD in a differential measurement mode. The temperatures of the graphite furnaces were pre-defined independently for creating a temperature difference between material ends and controlled by additional thermocouples. Temperature values were maintained by a PID control algorithm.

For all the studied structures, a created temperature gradient was directed within a plane of the layers (Fig. 3, *a*). Due to an extremely small thickness of the epitaxial layer, it is impossible to pre-define the temperature gradient in a perpendicular direction — along the normal to the surface. The thermo-EMF value was measured by same-name ends of the thermocouples attached to hot and cold ends of the sample and values of the temperatures at the sample ends were measured by the same thermocouples. In order to improve a thermal contact, the sample was pressed by the graphite clamps. Dielectric insulation between the sample and the furnace elements was provided by mica.

Resistivity measurement is realized by a standard four-contact diagram (Fig. 3, b): two wires (chromel and alumel) were pressed to contact pads of the sample: a current was transmitted through the chromel wires and voltage was recorded from the alumel wires. The wires were connected to a current/voltage source/meter Keithley240s. Table temperatures were set to be equal and when thermodynamic equilibrium was obtained, a current-voltage characteristic was recorded. A distance between the contacts is pre-defined to be equal to a sample width, thereby making it possible to calculate resistivity by the formula

$$\rho = R \cdot d, \tag{11}$$

where d is a thickness of the conducting layer. Since all the structures were grown on the non-conducting substrates of semi-insulating gallium arsenide, the thickness of the conducting layer will be understood to be a thickness of the formed film. In order to estimate the influence of the substrate on the thermoelectric properties of the film, the above-described procedure was used to study a temperature dependence of resistivity of the substrate. The thermoelectric characteristics were measured within the temperature range 350 – 800 K. The procedures of measurement of the Seebeck coefficient and resistivity can be additionally found in the studies [31–34].

4. Results and their discussion

Fig. 4 and 5 shows the experimental temperature dependences of the Seebeck coefficients and resistivity of the studies samples, respectively. The numbers of curves coincide with the numbers of the samples. A negative value of the Seebeck coefficient is recorded for the studied samples, which corresponds to donor conductivity of the epitaxial layers [1,2]. With an increase of the temperature, the value of the Seebeck coefficient increases in

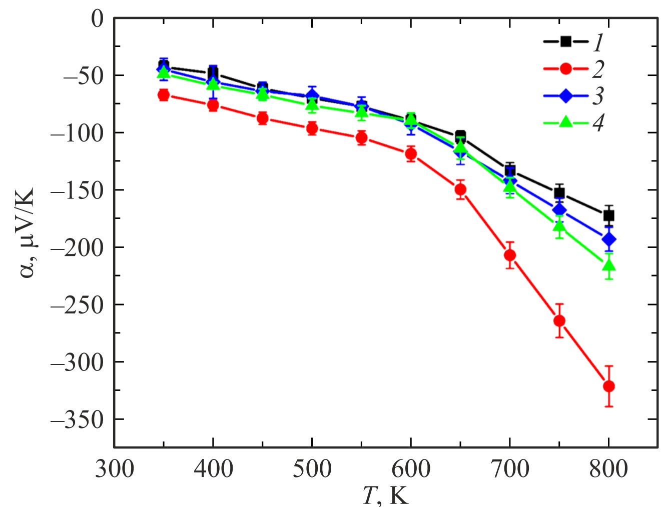

Figure 4. Experimental temperature dependence of the Seebeck coefficient of the studied samples.

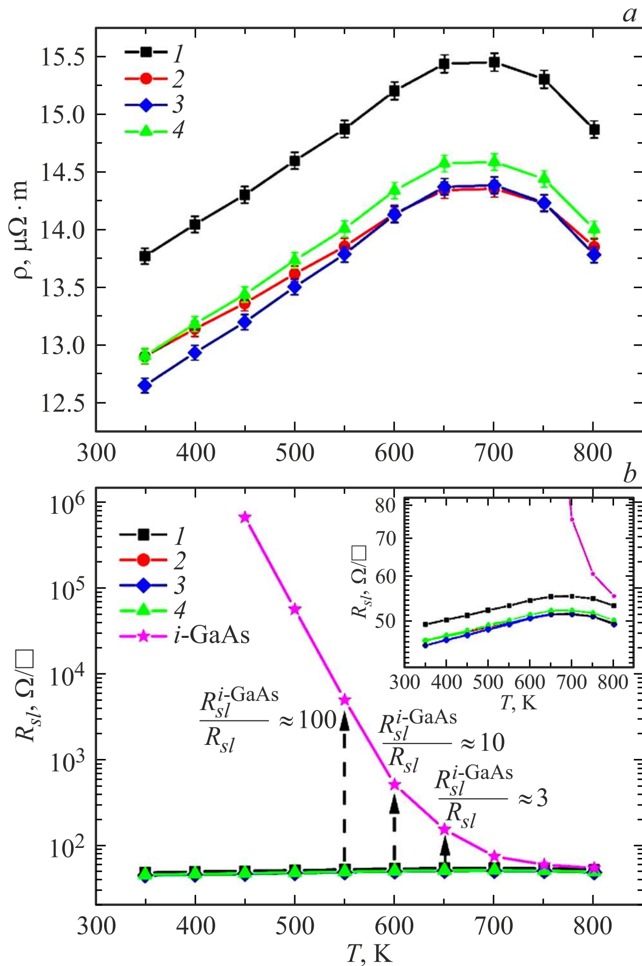

Figure 5. *a* — an experimental temperature dependence of resistivity of the studied samples, *b* — correlation of a layer resistance of the samples and the substrate of semi-insulating gallium arsenide.

absolute value. At the temperature above 600 K, all the studied structures exhibit an inflection at the temperature dependence $\alpha(T)$ and a sharp increase (in modulus) of the Seebeck coefficient. This special feature is explained by shunting of the epitaxial layer with the substrate of semi-insulating gallium arsenide. This fact is additionally confirmed by a maximum observed on the temperature dependence of resistivity within this temperature interval (Fig. 5, *a*). Presence of the maximum on the dependence $\alpha(T)$ usually corresponds to a point of transition to intrinsic conductivity of the material [1,2]. In the considered case, reduction of resistance at the temperatures above 600 K is related to a contribution by intrinsic conductivity of the substrate, whose resistivity exponentially decreases with a temperature increase.

Fig. 5, *b* compares the temperature dependence of layer resistances of the substrate and the studied samples in a semi-logarithmic scale. Whence, it is clear that when reaching the temperature of 600 K a difference of layer resistance of the substrate and resistance of any of the samples is just an order of the magnitude. With this difference, the contribution by the Seebeck coefficient of the substrate to the total value α already exceeds a measurement error. When the temperature increases to 650 K, the resistance ratio is several units. At 800 K, layer resistance of the substrate is comparable with the value obtained when measuring the samples, which is distinctly clear in an insert additionally shown in Fig. 5, *b*. Due to a significantly large thickness as compared to the nanoscale epitaxial layer, the thermoelectric characteristics of the substrate prevail at the temperatures above 600 K.

Based on results of the measurements of the temperature dependences of the Seebeck coefficient and resistivity of the samples, further analysis of the thermoelectric characteristics will be considered within the temperature range 350 – 600 K.

Within the said range of the temperatures, a kind of the dependences $\alpha(T)$ and $\rho(T)$ similar for all the studied samples (Fig. 4, 5).At the same time, for each measurement temperature the values of the Seebeck coefficient and electrical conductance are somewhat different from each taking into account the error. The recorded differences between the values of conductivity can be due to a technological spread of the thicknesses (since during the measurements the resistance value is related to the thickness of the epitaxial layer). The value of the technological spread is 10 % from structure to structure. On the contrary, the Seebeck coefficient values do not depend on the thickness within 10 % of the technological spread. Therefore, the recorded differences of the magnitude α are due to differences in a structure of the samples and, consequently, in parameters of the quantum-dimensional layer.

Thus, a difference of the studied structures from the reference one without QDs is that the latter has no quantum limitation for electrons along a direction of the created temperature gradient. Therefore, electrons even being localized in the quantum well can freely move along the direction of pre-definition of the temperature gradient and participate in processes of thermal and electrical conductivity. For the quantum dots, as for objects of a three-dimensional quantum limitation, motion of QD-localized electrons is limited, including along the direction of the temperature gradient, which affects values of the thermoelectric coefficients.

In order to estimate the contribution by localization of QD charge carriers to the recorded values of the Seebeck coefficient and electrical conductance, the experimental results were compared with the results obtained for the reference structure without a QD layer (the sample 1). Fig. 6 shows the temperature dependences of the difference thermo-EMF $(\alpha(T) - \alpha_c(T))$, where $\alpha_c(T)$ is a value of the Seebeck coefficient for the reference structure. Fig. 7 shows the temperature dependences of the magnitude $\rho_c(T)/\rho(T) = \sigma(T)/\sigma_c(T)$, where $\rho_c(T)$ is a value of resistivity for the reference structure, $\sigma(T)$ and $\sigma_c(T)$ are conductivity of the studied structures and the reference structure, respectively. The numbers of curves coincide with the numbers of the samples. The difference $\alpha(T) - \alpha_c(T)$

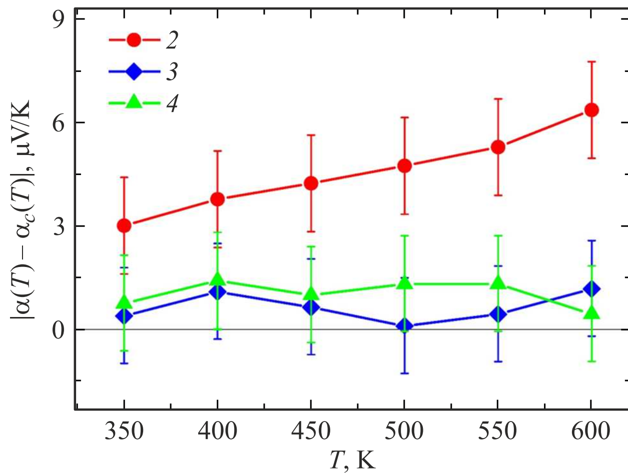

Figure 6. Temperature dependence of a modulus of the difference value of the Seebeck coefficient $|\alpha(T)-\alpha_c(T)|$, which is calculated by measurements within the operating range.

is selected for analysis due to the fact that in the first approximation the quantum dots make an additive contribution to the value of the Seebeck coefficient. At the same time, the QD contribution to the measured value of resistivity is not additive and, moreover, the values of ρ also depend on the technological spread of the thickness. For this reason, in order to estimate the QD influence on resistivity, the magnitude $\rho_c(T)/\rho(T)$ was selected.

It is clear from the graphs of $\alpha(T)-\alpha_c(T)$ that the values of the Seebeck coefficient for the studied and reference structures are the same (the difference does not exceed the measurement error) for all the samples except for the sample 2. For the said sample, an increase of the Seebeck coefficient is recorded to be approximately by $4\,\mu$V/K, which is about 10% of the value obtained for the reference structure. The differences between the values of resistivity (Fig. 5) have a more complicated nature and, as noted above, can be due to the technological spread of the thicknesses of the layers.

We not that the difference in the thicknesses of the layers does not depend on the measurement temperature. If the technological spread is the only factor inducing the difference of the resistance values, then the ratio $\rho_c(T)/\rho(T)$ would not depend on the temperature. Presence of the dependence of the magnitude $\rho_c(T)/\rho(T)$ on the measurement temperature, which is recorded in Fig. 7, is related by us to properties of the quantum-dimensional layer. Comparison of the measured values of ρ for the various temperatures makes it possible to estimate the contribution by the quantum-dimensional layer to current flowing and the value of resistivity.

Thus, for the sample 2 we have recorded a relative decrease of resistivity with an increase of the temperature as compared to the reference structure. We explain this effect by localization of charge carriers in the quantum dots at the low temperature. The QD-localized carriers are not involved in conductivity, since their movement is limited in all the three directions. As the temperature increases, the carriers are thermally emitted from the quantum dots. These carriers make an additional contribution to electrical conductance, which exactly causes reduction of resistivity as well as to the value of the Seebeck coefficient. The contribution by the carriers to electrical conductance and the Seebeck coefficient depends on the properties of the quantum-dimensional layer: the density of states at the dimensional quantization levels of the array of the quantum dots (which is determined by the number) and a value of a limiting potential.

One to the most common methods of experimental estimation of the structure of the energy levels and the value of the limiting potential in the quantum dots based on direct-band materials is PL spectroscopy [17–28]. The measurements of the temperature dependence of PL intensity also make it possible to estimate a value of thermal emission of the charge carriers from the quantum dots [38], which is the main process contributing to enhancement of the thermoelectric characteristics. The said measurements were performed for all the formed thermoelectric structures. The PL spectra of the sample 3, which are measured at the various temperatures, are exemplified in Fig. 8, *a*. The spectra exhibit peaks related to radiative transitions with involvement of the states localized in the quantum dots [27–29]. With the increase of the temperature, we observe a long-wavelength shift of the spectrum, which is related to reduction of a band gap of the materials, as well as reduction of FL integral intensity related to thermal emission of the charge carriers from the quantum dots.

Efficiency of thermal emission determines a number of the charge carriers that additionally contributing to the thermoelectric characteristics during heating. The efficiency can be estimated by the temperature dependence of PL intensity. Fig. 8, *b* shows a dependence of integral intensity (an area under the graph shown in Fig. 8, *a*) on a

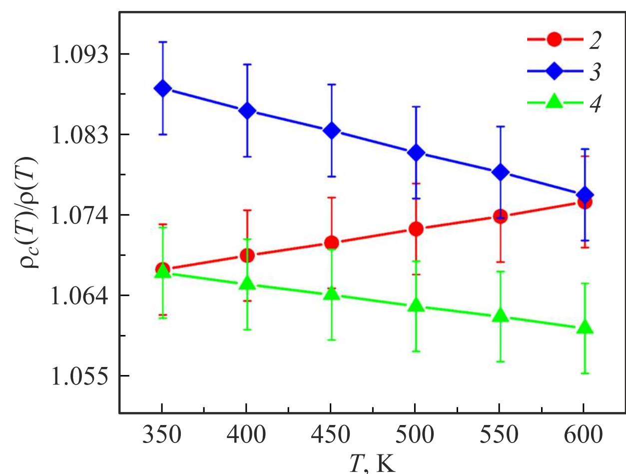

Figure 7. Temperature dependence of the ratio of resistivities of the studied and reference samples $\rho_c(T)/\rho(T)$.

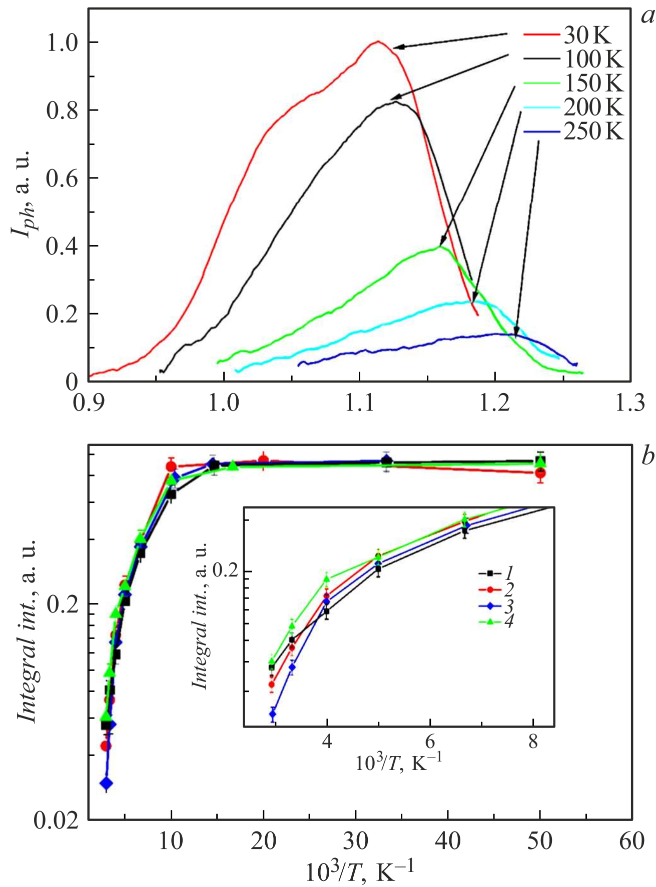

Figure 8. *a* — the PL spectra of the QD sample 3, which are measured within the temperature range 30 − 250 K. The temperature value for each curve is specified in the graph; *b* — the temperature dependences of PL integral intensity of the studied structures. The number of a curve corresponds to the number of the sample, the insert shows an enlarged portion of the high temperatures.

reciprocal temperature. Thermal emission is recorded by reduction of PL intensity at the temperatures above 80 K. According to the known studies [35–39], PL intensity in the heterostructures containing the quantum dots can be described by the formula

$$I \sim 1 + \Sigma_i \exp\left(-\frac{E_{ai}}{k_b T}\right), \quad (12)$$

where E_{ai} is energy of activation of the i-th mechanism of thermal emission of the carriers from the quantum dots. The quantum dots have a system of levels formed, which includes the 2D-levels in a quantum well, on which the quantum dots are formed, wherein the very quantum dots are characterized by a size spread. Therefore, several mechanisms of thermal emissions can function simultaneously [36–39], wherein each of them is characterized by its own value of energy of activation. The different mechanisms of emission can be effective at the various temperatures when a summand $\exp(-E_{ai}/kT)$ is close

Table 2. Calculated estimated values of efficiency energy

№	E_a, meV
1	5.5 ± 1.5
2	13.8 ± 2.5
3	9.1 ± 2.0
4	5.6 ± 1.5

to unit. For the studied structures, the largest interest is paid to the high-temperature range 300 − 600 K, for which the thermoelectric effect is recorded. However, due to limitations of a measurement system applied by us PL can be measured only for an initial portion of this range. Nevertheless, for correlating rates of reduction of PL intensity with the temperature increase it is possible to introduce an quantitative decay parameters for this portion (E_a), which is determined according to the relationship

$$I = I_0 \exp\left(\frac{E_a}{k_b T}\right). \quad (13)$$

Here the parameter E_a is calculated by approximating a final portion of the temperature dependence of PL integral intensity by the formula (13). A physical meaning of E_a is a certain value of energy of activation, which is averaged for all the processes of thermal emission from the quantum dots. It is this value that reflects the contribution by the QD-localized carriers to the thermoelectric effects, since this contribution provides emission from any localized states into a continuum. The calculated estimated values are given in Table 2. Comparison of the value of E_a for the various structures makes it possible to estimate efficiency of emission of the carriers from the quantum dots at increased temperatures.

It is clear that the value of E_a depends on conditions of structure manufacturing, i.e. exactly on the growth temperature. The highest value of E_a was obtained from the structure 2 formed at the growth temperature of 550 °C. The decrease of the temperature for the other structures results in a monotonic decrease of E_a. The least value is typical for the sample formed at the lowest temperature. The obtained value (5.6 ± 1.5) meV coincides with the value obtained for the reference structure without QDs. We underline that the largest value of energy of activation, which is obtained for the sample 2, well correlates with presence of an additional contribution to the magnitude α in this sample and with reduction of ρ. The obtained results agrees well with a suggested hypothesis on the contribution by thermal emission of the carriers from the quantum dots to the thermoelectric coefficients. The lower the limiting potential, the lower the concentration of the carriers localized at the dimensional quantization levels in the quantum dots at the increased temperature. In case of the high limiting

potential, the charge carriers remain localized in the quantum dots at the increased temperatures. Therefore, due to heating additional electrons are released, which increase the Seebeck coefficient and electrical conductance of the sample.

A lower boundary of the temperatures, at which the contribution of the localized carriers to the thermoelectric effects is recorded, is a point of start of thermal emission (based on the PL temperature dependence, this point is in the temperature range above 80 K). When the temperature gradient is created, a value of the concentration of conduction electrons at the hot end increases due to an additional contribution by thermal emission from the quantum dots — the concentration of the carriers localized in the quantum dots exponentially decreases with the temperature increase according to the formula (12). One shall expect enhancement of the thermoelectric effect within a temperature range, at which the quantum dots still have a relatively high concentration of the localized charge carriers. The upper temperature boundary of the effect is probably a point, at which there is full PL quenching in the QD area. It corresponds to a situation of the low concentration of the charge carriers localized in the quantum dots. It is obvious that the temperature range of enhancement 80 – 300 K depends on the value of the limiting potential. In all the structures with the low limiting potential, this range does not coincides with the temperature range 350 – 600 K, in which the thermoelectric effect was studied. An exception is the sample 2, for which a deeper limiting potential is obtained: in this case, even at the increased temperatures the quantum dots still have electrons that contribution to the thermo-EMF and electrical conductance.

Formation of the deeper limiting potential for the sample 2 as compared to the other samples is caused by selecting process modes of growth. It is known that the formation temperature affects a QD size and a degree of mixing of materials of the quantum dots and the matrix (InAs and GaAs, respectively). According to the study [39], when the quantum dots are formed by metalorganic vapour-phase epitaxy at the reduced pressure within the growth temperature range 520 °C – 550 °C, the QD size increases with a decrease of the growth temperature. The quantum dots formed at the temperature of 550 °C (similar to the sample 2) usually differ by higher sizes of nanoclusters as compared to the other samples of the series, for which the growth temperature was lower. In the larger-size nanoclusters the dimensional quantization level is shifted downwards by energy, while the value of the limiting potential increases [39]. Probably, these are the quantum dots that were formed in the sample 2, which exactly provided recorded enhancement of the thermoelectric effect.

An increase of the above-said coefficients in the sample 2 provides an increase of a value of the power factor as compared to the reference structure. Fig. 9 shows a temperature dependence of the power factor, which is calculated based on the obtained experimental data.

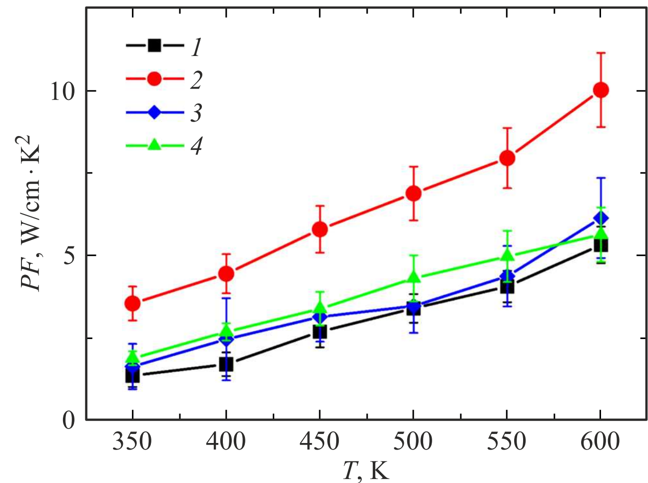

Figure 9. Calculated temperature dependence of the power factor of the studied samples.

The highest value of the power factor belongs to the sample 2 within the entire given temperature interval. The recorded values of the power factor for this sample are about in 1.5 times higher than the obtained values on the other samples investigated in the present study. We note that the achieved values of the power factor on the sample 2 are comparable with the best worldwide values for the thin films of such a composition, for example, those published in the study [40].

Conclusions

The study has theoretically analyzed a principal increasability of the thermoelectric characteristics by creating the semiconductor thin-film systems that contain an array of the self-organized quantum dots. It includes the studies of the temperature dependences of the Seebeck coefficient and electrical conductance of the multi-layer structures that contain the layers of the quantum dots and the quantum wells based on the InGaAs solid solution. It is shown that when the quantum dots are formed with the quite high limiting potential, the charge carriers can localize along the direction of the temperature gradient. Thermal emission of the localized carriers, which is confirmed by the PL studies, additionally contributes to the increase of the Seebeck coefficient and the increase of electrical conductance. As a result, it is shown that the thermal effect is enhanced in the QD structures, which is manifested in the increase of the power factor in up to 1.5 times as compared to the reference samples.

Funding

The study was financially supported by the Ministry of Education and Science of the Russian Federation within the scope of the State Assignment (project FSWR-2023-0037).

Conflict of interest

The authors declare that they have no conflict of interest.

References

[1] E. Macia-Barber. *Thermoelectric Materials: Advances and Applications* (Taylor & Francis Group, LLC, 2015)
[2] C. Gayner, K.K. Kar. Prog. Mat. Sci., **83**, 330 (2016). DOI: 10.1016/j.pmatsci.2016.07.002
[3] L.D. Hicks, T.C. Harman, X. Sun, M.S. Dresselhaus. Phys. Rev. B, **53** (16), R10493 (1996). DOI: 10.1103/physrevb.53.r10493
[4] H. Noro, K. Sato, H. Kagechika. J. Appl. Phys., **73**, 1252 (1993). DOI: 10.1063/1.353266
[5] B.C. Sales, D. Mandrus, R.K. Williams. Science, **272** (5266), 1325 (1996). DOI: 10.1126/science.272.5266.1325
[6] L.D. Ivanova, Yu.V. Granatkina. Inorg. Mater., **36** (7), 672 (2000). DOI: 10.1007/BF02758419
[7] H. Li, J. Feng, L. Zhao, E. Min, H. Zhang, A. Li, J. Li, R. Liu. Funct. Inorg. Mater. Devices, **16** (17), 22147 (2024). DOI: 10.1021/acsami.4c02141
[8] H.-L. Zhuang, J. Yu, J.-F. Li. Small Sci., **5** (3), 2400284 (2024). DOI: 10.1002/smsc.202400284
[9] P. Cervino-Solana, M.J. Ramirez-Peral, M.S. Martín-González, O. Caballero-Calero. Heliyon, **10** (16), e36114 (2024). DOI: 10.1016/j.heliyon.2024.e36114
[10] K. Luo, H. Chen, W. Hu, P. Qian, J. Guo, Y. Deng, L. Yang, Q. Sun, L. Liu, L. Cao, W. Qiu, J. Tang. Nano Energy, **128**, 109845 (2024). DOI: 10.1016/j.nanoen.2024.109845
[11] X. He, C. Li, S. Zhu, J. Cai, G. Yang, Y. Hao, Y. Shi, R. Wang, L. Wang, X. Li, X. Qin. Chem. Eng. J., **490**, 151470 (2024). DOI: 10.1016/j.cej.2024.151470
[12] X. Chen, Z. Zhang. Build. Environ, **253**, 111276 (2024). DOI: 10.1016/j.buildenv.2024.111276
[13] Q. Jiang, Y. Wan, Y. Qin, X. Qu, M. Zhou, S. Huo, X. Wang, Z. Yu, H. He. Adv. Fiber Mater., **2**, 3 (2024). DOI: 10.1007/s42765-024-00416-6
[14] Y. Cui, X. He, W. Liu, S. Zhu, M. Zhou, Q. Wang. Adv. Fiber Mater., **6**, 170 (2024). DOI: 10.1007/s42765-023-00339-8
[15] M. Magno, D. Brunelli, L. Sigrist, R. Andri, L. Cavigelli, A. Gomez, L. Benini. Sustain. Comput.: Inform. Syst., **11**, 38 (2024). DOI: 10.1016/j.suscom.2016.05.003
[16] M. Takashiri, T. Shirakawa, K. Miyazaki, H. Tsukamoto. Sens. Actuators A: Phys., **138** (2), 329 (2007). DOI: 10.1016/j.sna.2007.05.030
[17] P. Sun, B. Wei, J. Zhang, J.M. Tomczak, A.M. Strydom, M. Sondergaard, B.B. Iversen, F. Steglich. Nat. Commun., **6**, 7475 (2015). DOI: 10.1038/ncomms8475
[18] J. Mao, Z. Liu, Z. Ren. Quantum Mater., **1**, 16028 (2016). DOI: 10.1038/npjquantmats.2016.28
[19] J.P. Heremans, V. Jovovic, E.S. Toberer, A. Saramat, K. Kurosaki, A. Charoenphakdee, S. Yamanaka, G.J. Snyder. Science, **321**, 554 (2008). DOI: 10.1126/science.1159725
[20] A. Khitun, K.L. Wang, G. Chen. Nanotechnology, **11**, 327 (2000). DOI: 10.1088/0957-4484/11/4/327
[21] M. Cutler, N.F. Mott. Phys. Rev., **181** (3), 1336 (1969). DOI: 10.1103/PhysRev.181.1336
[22] M.V. Maximov, A.M. Nadtochiy, S.A. Mintairov, N.A. Kalyuzhnyy, N.A. Kalyuzhnyy, N.V. Kryzhanovskaya, E.I. Moiseev, N.Yu. Gordeev, Y.M. Shernyakov, A.S. Payusov, F.I. Zubov, V.N. Nevedomskiy, S.S. Rouvimov, A.E. Zhukov. Appl. Sci., **10**, 1038 (2020). DOI: 10.3390/app10031038
[23] A.V. Zdoroveishchev, P.B. Demina, B.N. Zvonkov. Vestnik Nizhegorodskogo un-ta, **5**, 19 (2008) (in Russian).
[24] M.V. Dorokhin, S.V. Zaitsev, A.V. Rykov, AVB. Zdoroveishchev, E.I. Malysheva, Yu.A. Danilov, V.I. Zubkov, D.S. Frolov, G.E. Yakovlev, A.V. Kudrin. ZhTF, **87** (10), 1539 (2017) (in Russian). DOI: 10.21883/jtf.2017.10.44999.1989
[25] M.V. Dorokhin, P.B. Demina, A.V. Zdoroveishchev, S.V. Zaitsev, A.V. Kudrin. ZhTF, **92** (5), 724 (2022) (in Russian). DOI: 10.21883/JTF.2022.05.52377.302-21
[26] N.V. Baidus', P.B. Demina, M.V. Dorokhin, B.N. Zvonkov, E.I. Malysheva, E.A. Uskova. FTP, **39** (1), 25 (2005) (in Russian).
[27] I.A. Karpovich, S.B. Levichev, S.V. Morozov, B.N. Zvonkov, D.O. Filatov, A.P. Gorshkov, A.Yu. Ermakov. Nanotechnology, **13** (4), 445 (2002). DOI: 10.1088/0957-4484/13/4/301
[28] A.V. Zdoroveishchev, P.B. Demina, B.N. Zvonkov. Pis'ma v ZhTF (in Russian), **35** (2), 15 (2009).
[29] I.A. Karpovich, A.V. Zdoroveishchev, S.V. Tikhov, P.B. Demina, O.E. Khapugin. FTP, **39** (1), 45 (2005) (in Russian).
[30] A. Deh'e, D. Pavlidis, K. Hong, H.L. Hartnagel. IEEE Trans. Electron Devices, **44** (7), 1052 (1997). DOI: 10.1109/16.595931
[31] L.A. Mochalov, Yu.M. Kuznetsov, M.V. Dorokhin, D.G. Fukina, A.V. Knyazev, M.A. Kudryashov, Yu.P. Kudryashova, A.A. Logunov, O.V. Mukhina, A.V. Zdoroveyshchev, D.A. Zdoroveyshchev. Thin Solid Films, 752, 139244 (2022). DOI: 10.1016/j.tsf.2022.139244
[32] M.V. Dorokhin, Yu.M. Kuznetsov, P.B. Demina, I.V. Erofeeva, A.Yu. Zavrazhnov, M.S. Boldin, E.A. Lantsev, A.A. Popov, A.V. Boryakov, A.V. Zdoroveyshchev, M.V. Ved. Nanoscale Microscale Thermophys. Eng., **27** (2), 125 (2023). DOI: 10.1080/15567265.2023.2198581
[33] Yu.M. Kuznetsov, L.A. Mochalov, M.V. Dorokhin, D.G. Fukina, M.A. Kudryashov, Y.P. Kudryashova, A.V. Zdoroveyshchev, D.A. Zdoroveyshchev, I.L. Kalentyeva, R.N. Kriukov. Coatings, **13** (6), 1030 (2023). DOI: 10.3390/coatings13061030
[34] M.V. Dorokhin, Yu.M. Kuznetsov, P.B. Demina, I.V. Erofeeva, A.V. Zdoroveyshchev, M.V. Ved', D.A. Zdoroveyshchev, A.Yu. Zavrazhnov, I.N. Nekrylov, S.M. Peshcherova, R.V. Presnyakov, N.V. Sakharov. Inorg. Mater.: Appl. Res., **15**, 289 (2024). DOI: 10.1134/S207511332402014X
[35] S. Sanguinetti, M. Henini, M.G. Alessi, M. Capizzi, P. Frigeri, S. Franchi. Phys. Rev. B, **60** (11), 8276 (1999). DOI: 10.1103/PhysRevB.60.8276
[36] A. Chahboun, M.I. Vasilevskiy, N.V. Baidus, A. Cavaco, N.A. Sobolev, M.C. Carmo, E. Alves, B.N. Zvonkov. J. Appl. Phys., **103**, 083548 (2008). DOI: 10.1063/1.2913179
[37] E.C. Le Ru, J. Fack, R. Murray. Phys. Rev. B, **67**, 245318 (2003). DOI: 10.1103/PhysRevB.67.245318

[38] S. Sanguinetti, M. Padovani, M. Gurioli, E. Grilli, M. Guzzi, A. Vinattieri, M. Colocci, P. Frigeri, S. Franchi. Appl. Phys. Lett., **77**, 1307 (2000). DOI: 10.1063/1.1290385

[39] K. Sears, S. Mokkapati, H.H. Tan. In Z.M. Wang (editor). *Self-Assembled Quantum Dots* (Springer, 2008), p.359−403.

[40] T. Meng, X. Zhang, J. Yao, W. Zhang, H. Zhong, H. Zhu, Y. Zhang, H. Zhang, P. Zhang, H. Lu, Y. Zhao. Appl. Phys. Lett., 125, 044003 (2024). DOI: 10.1063/5.0213563

Translated by M.Shevelev